Preparation, characterization and catalytic properties of the microporous titanosilicate, ETS-10

TAPAN Kr DAS, A J CHANDWADKAR and S SIVASANKER

Catalysis Division, National Chemical Laboratory, Pune 411 008, India

Abstract. ETS-10 is a novel large pore (12 membered ring) molecular sieve containing Ti^{4+} in O_h environment and Si^{4+} in T_d environment sharing common O^{2-} ions. As a result, ETS-10 possesses large ion-exchange and adsorption properties, besides being acidic in the H-form. We report our studies on its synthesis, characterization using SEM, IR, TGA/DTA, UV-VIS, MAS-NMR techniques, adsorption and catalytic properties.

Keywords. Titanosilicate; synthesis of ETS-10; characterization of ETS-10; catalytic properties of ETS-10.
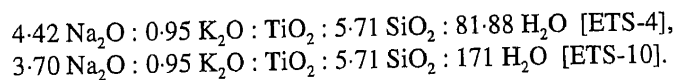
1. Introduction

A new family of titanium silicate molecular sieves was recently discovered at Engelhard (Kuznicki 1990; Kuznicki *et al* 1991). These materials called ETS-4 and ETS-10 have unique molecular architecture due to octahedrally coordinated titanium framework ions. The structure of ETS-10 is an open three-dimensional one consisting of chains of Ti^{4+} octahedra linked to classical tetrahedral silica rings (Anderson *et al* 1994). A three-dimensional network of the interconnecting channels intersect a central pore (8 Å diameter). ETS-10 has a significant ion exchange capacity (2 Na^+ or 2 K^+ per Ti^{4+}) and the protonic form is moderately acidic.

In the present paper, we report our studies on the synthesis of ETS-10 using seeds of ETS-4, its characterization and catalytic properties in the dehydration of alcohols and isomerization of 1-butene and *m*-xylene.

2. Experimental

Synthesis of the titanosilicate (ETS-10) using seeds of ETS-4 was carried out hydrothermally using sodium silicate, titanium trichloride solution (15% solution in HCl, Loba Chemie, Bombay), sodium hydroxide, potassium fluoride dihydrate (GR Loba Chemie, Bombay) and seeds of ETS-4 (titanosilicate having small pore size 4 Å) prepared as reported earlier (Kuznicki *et al* 1991; Anderson *et al* 1994).

The molar composition of the gel in terms of oxides was as follows:

$$4\cdot 42\, Na_2O : 0\cdot 95\, K_2O : TiO_2 : 5\cdot 71\, SiO_2 : 81\cdot 88\, H_2O \ [ETS\text{-}4],$$
$$3\cdot 70\, Na_2O : 0\cdot 95\, K_2O : TiO_2 : 5\cdot 71\, SiO_2 : 171\, H_2O \ [ETS\text{-}10].$$

The synthesis of ETS-4 and ETS-10 were carried out as follows:

(i) *Synthesis of ETS-4 (seed)*: A solution of sodium silicate was added to NaOH with stirring. Titanium trichloride ($TiCl_3$ 15% solution in HCl) was added dropwise to the above mixture and stirred for 30 min to get a blackish paste. Potassium

fluoride dihydrate ($KF \cdot 2H_2O$) was next added to the mixture and stirred for 1 h at room temperature to get a homogeneous gel (pH = ~ 11·0). This gel was transferred to a stainless steel autoclave and capped tightly and crystallization carried out at 423 K for 5–10 days. After crystallization the solid material was filtered off and washed with deionized water. The product was then dried and identified as the crystalline small pore titanosilicate (ETS-4) with the X-ray diffraction pattern presented in figure 1A.

(ii) *Synthesis of ETS-10 using seeds of ETS-4*: A solution of sodium silicate in distilled water was mixed with NaOH with stirring. Titanium trichloride (15% solution in HCl) was then added dropwise to the above stirred gel. The paste like blackish material was allowed to stir for 30 min. $KF \cdot 2H_2O$ was next added to the above paste and stirred well. Finally ETS-4 (seed, 6·99%) was added and stirred vigorously for another 60 min till it was homogeneous (pH = 10·8–11·0) at room temperature. The gel was transferred to a stainless steel autoclave and crystallized at 443 K for 10 days as mentioned above. The washed crystalline product was identified as the large pore titanosilicate (ETS-10) with the X-ray diffraction pattern presented in figure 1B.

The crystalline phase identification and phase purity of the sample was verified by X-ray diffraction (Rigaku, Model D-max III). The chemical composition of the samples was determined by a combination of wet chemical methods and atomic absorption spectroscopy (Hitachi Model Z-8000). Their average particle size and morphology were determined by scanning electron microscopy (JEOL, JSM 5200). The UV-VIS diffuse reflectance spectra of the samples were obtained by using a Shimadzu (Model UV-210PC) spectrometer. FTIR spectra were recorded with a Nicolet FTIR spectrometer (Model 60XB). The solid state MAS NMR ^{29}Si and ^{23}Na were recorded at 295 K using a Bruker MSL-300 FT NMR spectrometer. Bloch decays were averaged 2400 times before Fourier transformation to obtain
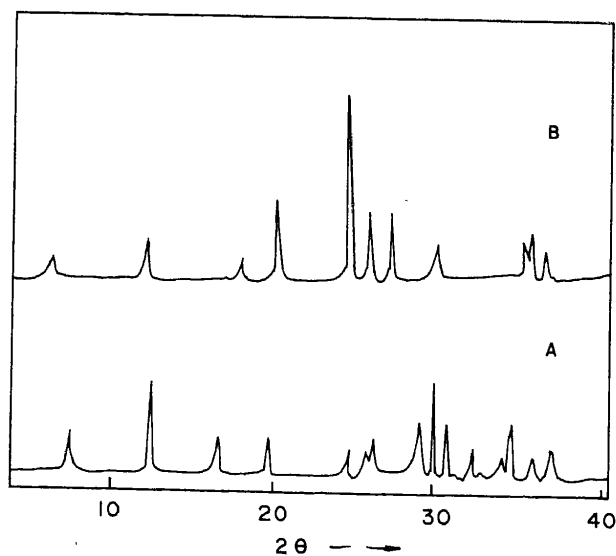

Figure 1. XRD patterns of the as-synthesized titanosilicates: (A) ETS-4 and (B) ETS-10.

spectra with sufficient S/N. While acquiring [29]Si spectra, a recycle time of 4s was found to be sufficient to give fully relaxed spectra. [29]Si spectra were measured using TMS as the primary reference. ^{29}Si NMR spectra were recorded at $\gamma = 59.6$ MHz. An excitation pulse (t pulse) of 2 μs was used with 2000 NS (no. of scans). While acquiring [23]Na spectra, a recycle time of 1 s was found to be sufficient to give fully relaxed spectra. [23]Na spectra were measured using sodium chloride as the primary reference. [23]Na spectra were recorded at 79·39 MHz. An excitation pulse of 2 μs was used with 200 NS.
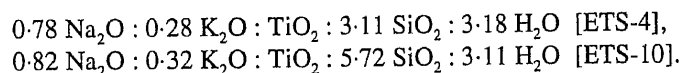
The zeolite samples of different crystallinity were also further characterized by the adsorption of different probe molecules using a vacuum (Cahn) electrobalance. Prior to sorption measurements, about 200 mg of the sample was activated at 573 K under vacuum. The ion-exchange property of the titanosilicate (ETS-10) was evaluated with 1·0 N (NaCl + KCl) mixture and then ion exchanging further with 2–3 N ammonium nitrate solution. The exchange was done under reflux for 2 h. The procedure was repeated to ensure complete ion-exchange.

The catalytically active protonic form of the titanosilicate [H-ETS-10] was obtained by repeated ion-exchange (till Na and K levels were less than 80 and 50 ppm respectively in the solid) with 1 N solution of ammonium nitrate (wt of solution/wt of zeolite = 10). The final product was filtered, dried (in an air oven at 383 K for 10 h) and calcined stepwise at 623 K for 35–40 h in a flow of nitrogen and then air.

3. Results and discussion

3.1 *Synthesis of ETS-4 and ETS-10*

Chemical analysis of the synthesized samples are given below:

$$0.78 \ Na_2O : 0.28 \ K_2O : TiO_2 : 3.11 \ SiO_2 : 3.18 \ H_2O \ [\text{ETS-4}],$$
$$0.82 \ Na_2O : 0.32 \ K_2O : TiO_2 : 5.72 \ SiO_2 : 3.11 \ H_2O \ [\text{ETS-10}].$$

The X-ray diffraction patterns of the titanosilicates ETS-4 and ETS-10 shown in figure 1 match very closely with those published earlier (Kuznicki 1990; Kuznicki *et al* 1991; Anderson *et al* 1994). The relative crystallinity of the sample was calculated by comparing the area of peak in the range of $2\theta = 24.65–27.5°$ to that of the most crystalline reference materials (ETS-10) obtained from the same batch composition.

To study the effect of temperature on the formation of the titanosilicate, the kinetics of crystallization were studied in the range 423–473 K by comparing the extent of crystallization of the gel mixture at different intervals of synthesis time. The extent of crystallization was estimated from the ratios of the sum of the areas of the intense XRD peaks of the sample under consideration to that of the most crystalline sample obtained during the study (Domine and Quobex 1968; Tsitsishvilli *et al* 1979; Chao *et al* 1981). The curves (based on XRD estimation of crystallinity) for the crystallization kinetics of ETS-10 for the gel composition mentioned earlier are presented in figure 2. The curves typically exhibit a sharp continuous rise of crystallization. The intercept made by the curve on the time axis (abscissa) is defined as the induction period (the time needed to form crystallization centers or

nuclei). In accordance with thermodynamic expectations, it is found from figure 2 that the induction period is inversely proportional to the temperature. The rate of nucleation may be assumed to be proportional to the reciprocal of the induction period and hence, it varies directly with the crystallization temperature. The induction period is followed by the rapid formation of crystalline material i.e. the rate of crystallization increases rapidly with time up to about 60–70% crystallinity and then slows down.

Linear plots were obtained when the data were fitted into Avrami–Erofeev equation (Kulkarni *et al* 1982). Applying the Arrhenius equation, the activation energy values for nucleation (E_n) and crystallization (E_c) were found out to be 76·5 and 38·3 KJ mol^{-1}, respectively. Recently shortcomings of the applicability of the above equation to zeolite crystallization data has been pointed out (Thompson 1992). He has proposed that these Avrami–Erofeev transformation kinetics should be viewed as providing only a qualitative interpretation of zeolite crystallizations. Therefore, no meaningful deductions should be drawn from these linear plots. The futility of the assumptions were explained (Den Ouden and Thompson 1992) to arrive at the rate of nucleation and crystal growth for the applicability of the Arrhenius equation to evaluate the apparent activation energies for the nucleation (E_n) and crystal growth (E_c) process.

3.2 Characterization studies

3.2a SEM analysis: SEM photographs show that the small pore titanosilicate (ETS-4) used as seed in the present study has very irregular undefined particles ranging in size from 1–8 μm (figure 3a). On the other hand, ETS-10 synthesized (with $H_2O/SiO_2 = 30$) using ETS-4 seeds (6·99 wt% based on SiO_2 input) crystallizes as sharp, twinned cuboids in the size range 1–4 μm (figure 3b).
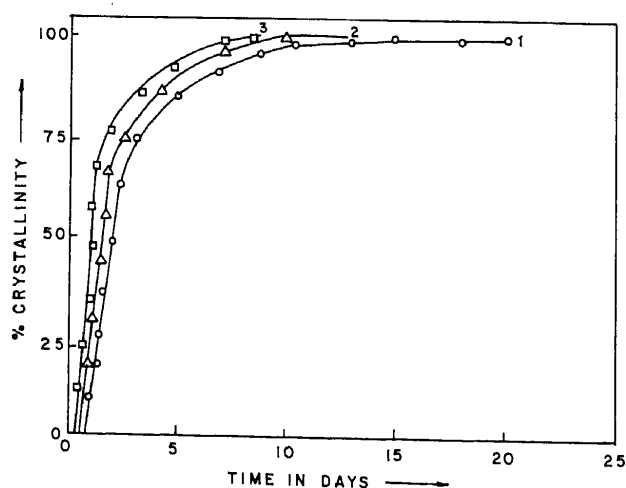

Figure 2. Effect of temperature on the kinetics of crystallization of ETS-10, Curves 1–3 correspond to 423 K, 443 K and 473 K, respectively.
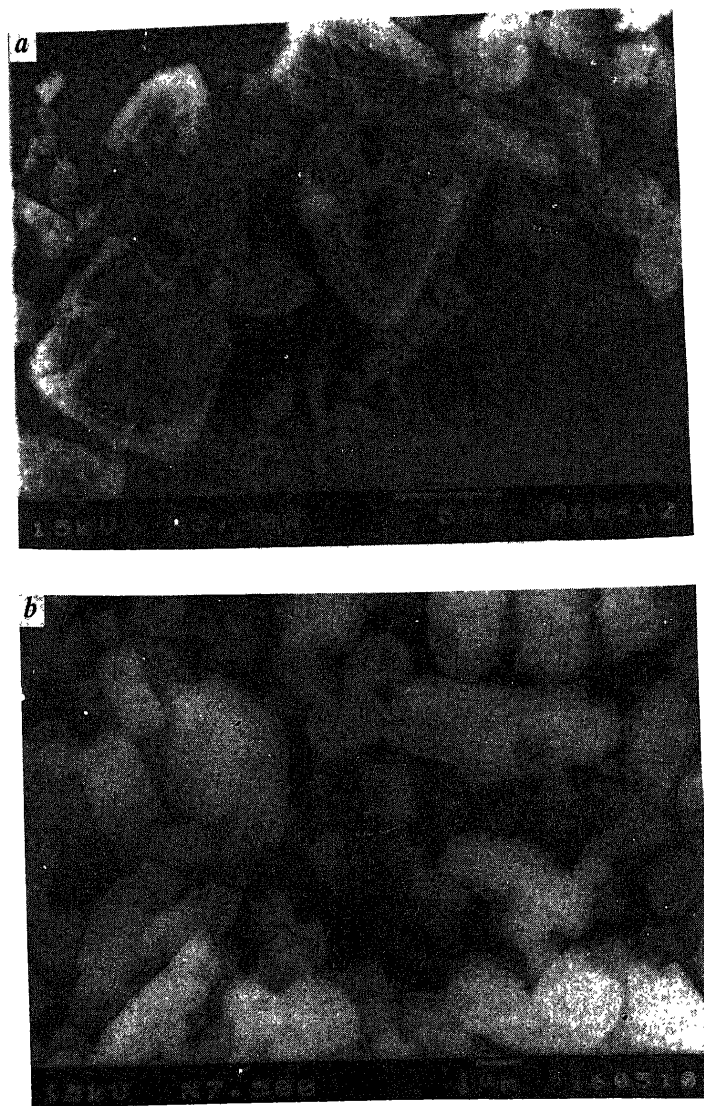
Figure 3. SEM photographs of titanosilicates: (a) ETS-4 (seed) and (b) ETS-10.

3.2*b* *IR studies*: The framework IR spectra (in the region 450–1300 cm^{-1}) of ETS-4 and ETS-10 are shown in figure 4 (curves A and B respectively). ETS-4 shows a prominent band at 1000 cm^{-1} and two weak absorptions at 1100 and 920 cm^{-1}. The positions of the major absorption bands and shoulders corresponding to the different symmetric and asymmetric stretching vibrations (Flanigen and Khatami 1971) remained almost unchanged (± 5 cm^{-1}) for the titanosilicates prepared using seeds. The FTIR spectra of surface hydroxyl groups in dehydrated ETS-10 is shown in figure 5. The peak around 3735 cm^{-1} is due to isolated terminal silanol groups (Chandwadkar *et al* 1993). The sharp peak at 3700 cm^{-1} observed on ETS-10
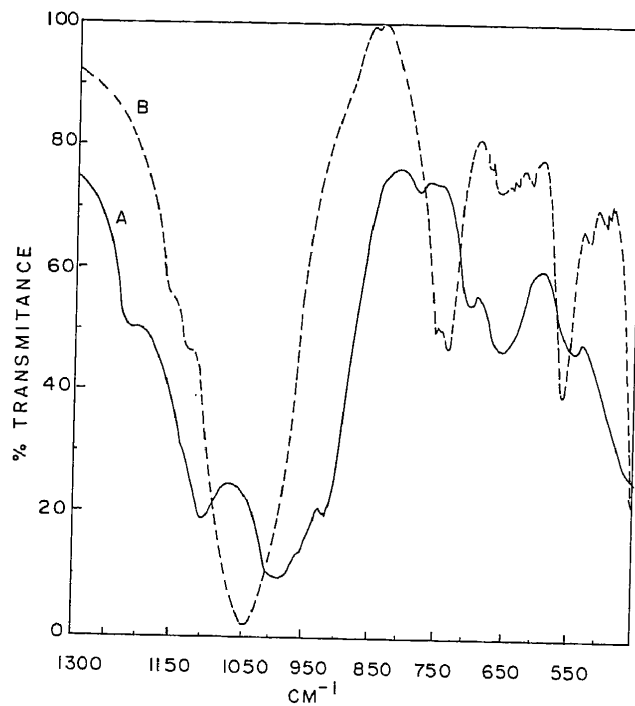
Figure 4. IR framework vibration spectra of the titanosilicates; (A) ETS-4 and (B) ETS-10.

probably is due to isolated Ti–OH groups. The broad band around 3200–3600 cm^{-1} is probably due to H-bonded surface hydroxyl groups of both Si and Ti.

3.2c TGA/DTA: The thermal behaviour of ETS-10 is shown in figure 6. The endotherm at 393 K is due to the loss of physically sorbed or occluded water, and at ~963 K may be due to the dehydration of terminal –OH groups. The two exotherms with peak maxima at 573 and 723 K are probably due to phase transitions.

3.2d UV-VIS (DRS): The diffuse reflectance spectra in the UV-VIS region of ETS-10 and ETS-4 are presented in figure 7 (curves a and b respectively). The broad absorption in the region 250–320 nm suggest the presence of Ti^{4+} in O$_h$ co-ordination (Jacobs 1992).

3.2e MAS-NMR: The ^{29}Si NMR spectrum of ETS-10 (figure 8A) shows three sharp bands at δ = −94·4(1), −96·8(2) and −103·8(3) ppm, indicating the presence of at least three different Si environments in ETS-10. The weak band at δ = −90·74 ppm (marked by an arrow) is probably due to ETS-4 present as an impurity in the sample as this band was prominent in the case of pure ETS-4. Further this band disappeared after calcination at 623 K.

The ^{23}Na NMR spectrum (figure 8B) shows the presence of two resonance bands at δ = 9·17(1) and −9·90(2) ppm corresponding to their presence in two different environments (Engelhardt and Michel 1987).
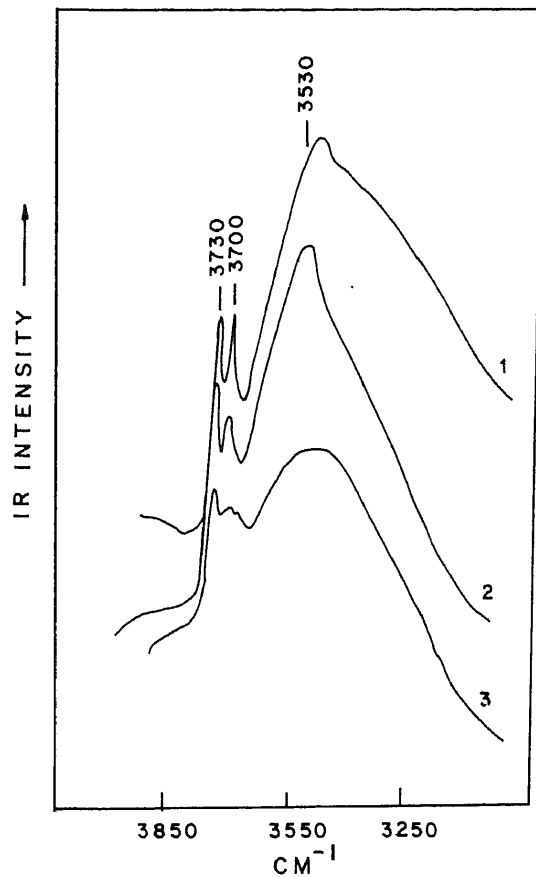
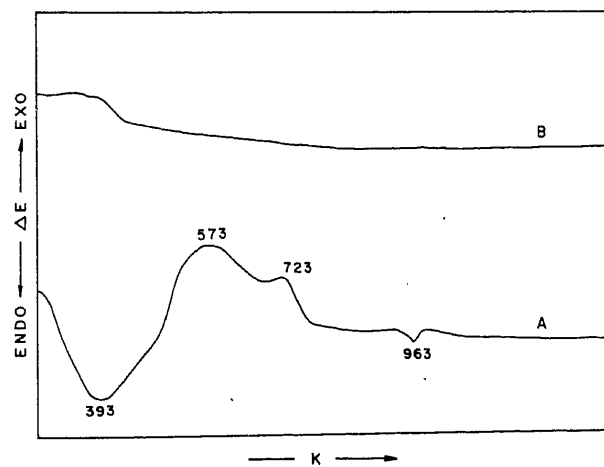**Figure 5.** FTIR spectra of ETS-10 recorded at 313 K, 373 K and 473 K (curves 1-3 respectively).

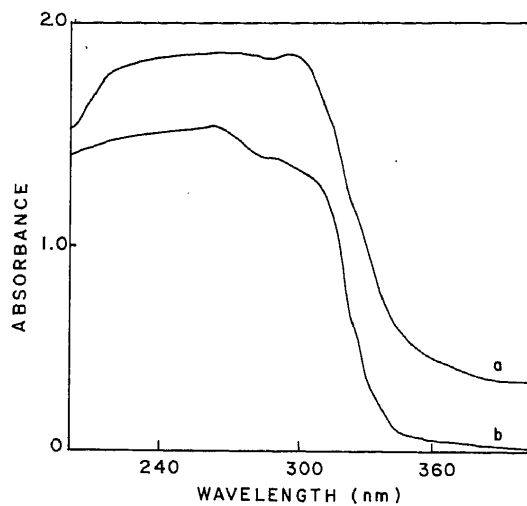**Figure 6.** Thermoanalytical curves of ETS-10: (A) DTA and (B) TGA.

Figure 7. UV-VIS diffuse reflectance spectra of titanosilicate samples: (a) ETS-10 and (b) ETS-4.
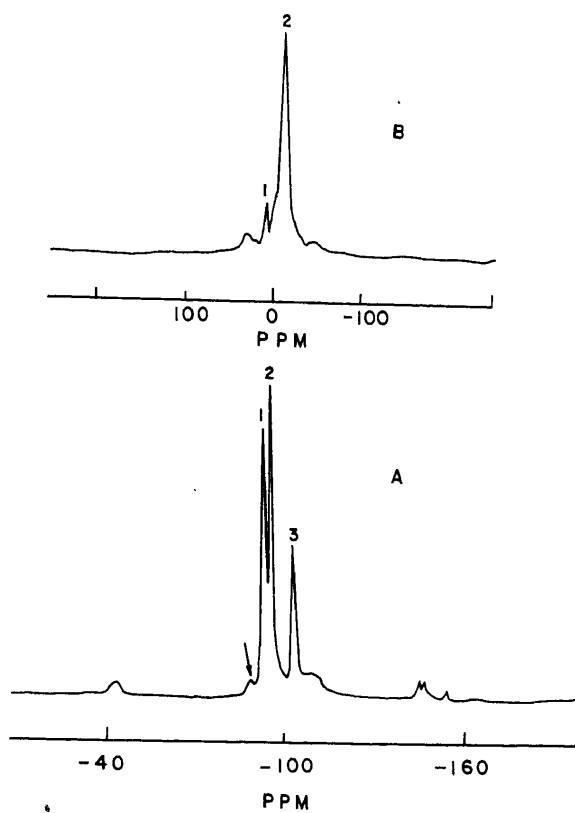

Figure 8. ^{29}Si and ^{23}Na MAS-NMR (curves A and B, respectively) of ETS-10.

3.2f *Sorption studies:* The sorption isotherms for water, *n*-hexane and 1,3,5-trimethylbenzene obtained at 298 K at a $p/p_0 = 0.5$ are presented in figure 9. The large adsorption capacity for water shows that the molecular sieve is hydrophilic in nature. Besides, the rapid adsorption in large amounts of 1,3,5-trimethylbenzene (diameter $= 8.4$ Å) confirms that ETS-10 has pores of diameter of at least 8 Å.

3.3 Catalytic studies

3.3a *Alcohol dehydration:* H-ETS-10 is active in the dehydration of alcohols. In the case of dehydration of alcohols it decreases in the order: *t*-butanol > cyclohexanol > isobutanol > 2-butanol > 1-butanol. The order of reactivities follows the same trend as the stabilities of the carbenium ions formed from them. The primary product of dehydration of isobutanol isomerizes further into 1- and 2-butenes. However, the isomerization is not significant when *t*-butanol is dehydrated. The dehydration of cyclohexanol leads mainly to cyclohexene and methyl-cyclopentenes (MCP⁼), the latter products being formed by the skeletal rearrangement of cyclohexene (table 1).

3.3b *Isomerization:* ETS-10 isomerizes 1-butenes, with the formation of large quantities of saturated compounds (butanes 57%). This shows that ETS-10 possess good hydrogen transfer activity. The excess hydrogen probably comes from the carbonaceous residues which were also formed in significant quantities.

The conversion of *m*-xylene over ETS-10 is moderate (16·4%). The low I/D ratio (isomerization/disproportionation $\simeq 0.5$) shows that not only are the pores of ETS-10 large but also its acid site density is very high leading preferentially to bimolecular disproportionation reactions instead of isomerization reactions (table 2). High acid
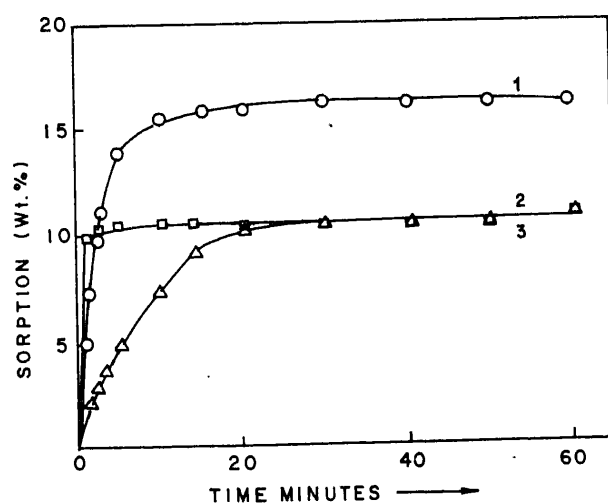

Figure 9. Sorption isotherms of H₂O, n-hexane and 1,3,5-trimethylbenzene (curves 1, 2 and 3 respectively) obtained over ETS-10.

Table 1. Dehydration of alcohols over ETS-10.

	1-butanol	2-butanol	Isobutanol	*t*-butanol	Cycolhexanol
Conv. (%)	87·9	90·6	99·9	99·9	99·9
Products wt. (%)					
i-Butene	0·11	1·4	1·2	0·18	–
Butene-1	17·2	7·2	10·4	–	–
i-Butene	2·5	48·0	54·5	98·8	–
n-Butane	0·5	0·24	0·22	–	–
t-Butene–2	36·8	15·5	17·7	0·26	
c-Butene-2	28·1	11·9	13·7	0·2	–
Cyclohexene	–	–	–	–	80·1
MCP*	–	–	–	–	18·4
C$_1$-C$_3$ and others	2·7	6·4	2·1	0·5	0·9

Temp.: 573 K, WHSV: 2 (h^{-1}), N$_2$: (5 ml/min), Press.: 1 atm. TOS: 1 h
*Methyl cyclopentenes.

Table 2. Isomerization activities of ETS-10.

1-Butene		*m*-Xylene	
Conv. (%)	98·6	Conv. (%)	16·4
Products wt. (%)		Products wt. (%)	
C$_1$–C$_3$	6·9	Benzene	1·9
i-Butane	43·5	Toluene	4·1
i-Butene	2·8	*p*-Xylene	1·0
n-Butane	13·3	*o*-Xylene	3·3
t-Butane-2	2·6	1,3,5 TMB*	1·3
c-Butane-2	1·8	1,2,4 TMB*	3·6
i-Pentane	18·7	1,2,3 TMB*	0·4
Others	9·0	Others	0·8

Temp.: 573 K, WHSV: 1 (h^{-1}), N$_2$: (5 ml/min), Press.: 1 atm. TOS: 1 h
*Trimethylbenzenes.

site density is due to the fact that concentration of the Ti^{4+} ions is high and each Ti^{4+} ion can lead to two acid sites.

4. Conclusions

ETS-10 can be suitably synthesized using ETS-4 as seeds. Infrared and UV-VIS(DRS) studies show that the Ti^{4+} ions are in O$_h$ symmetries in ETS-10 as reported by earlier workers. Adsorption studies reveal that the molecular sieve is hydrophilic and has pores of diameter of at least 8 Å. ETS-10 is found to be active in the dehydration of alcohols and the isomerization of 1-butene and *m*-xylene.

References

Anderson M W, Terasaki O, Ohsuna T, Phillippou T, Mackay S P, Ferreira A, Rochca J and Lidlin S 1994 *Nature (London)* **367** 347

Chandwadkar A J, Abdulla R A, Hegde S G and Nagy B 1993 *Zeolites* **13** 470

Chao K J, Tasi T C, Chen M S and Wang I 1981 *J. Chem. Soc. Faraday. Trans. I*, **77** 547

Den Ouden C J J and Thompson R W 1992 *Ind. Eng. Chem. Res.* **31** 369

Domine D and Quobex J 1968 *Molecular sieves* (London: Soc. Chem. Ind) p. 78

Engelhardt G and Michel D 1987 *High resolution solid state NMR of silicates and zeolites* (Chichester: John Wiley and Sons)

Flanigen E M and Khatami H 1971 *Mol. Sieve Zeolites I, Adv. Chem. Ser.* **101** 201 (Washington D.C.: American Chemical Society)

Jacobs P A 1992 *DGMK Tangenbericht* **171** 9204

Kulkarni S B, Shiralkar V P, Kotasthane A N, Borade R B and Ratnasamy P 1982 *Zeolites* **2** 313

Kuznicki S M 1990 US Patent 4,938,939

Kuznicki S M, Madon R J, Koermer G S and Thrust K A 1991 European Patent 405978

Thompson R W 1992 *Zeolites* **12** 680

Tsitsishvilli G V, Krupenikov A Yu, Mamulashvili M V and Urushadze M V 1979 *Russ. J. Phys. Chem.* **53** 975